A Testbed of Performance Evaluation for Fingerprint Based WLAN Positioning System

Wanlong Zhao, Shuai Han, Weixiao Meng and Deyue Zou
Communication Research Center, Harbin Institute of Technology
Harbin, China
[e-mail: zhaowanlong001@sina.cn, hanshuai@hit.edu.cn, wxmeng@hit.edu.cn, zoudeyue_hit@163.com]
*Corresponding author:Shuai Han

Received July 2, 2015; revised February 11, 2016; revised March 30, 2016; accepted April 20, 2016; published June 30, 2016

Abstract

Fingerprint positioning is a main stream and key technique for seamless positioning systems. In this paper, we develop a performance evaluation testbed for fingerprint based Wireless Local Area Network (WLAN) positioning system. The testbed consists of positioning server, positioning terminal, Access Point (AP) units, positioning accuracy analysis system and testing scenarios. Different from other testbeds tended to focus on testing in same situation, in the proposed testbed, a couple of scenarios are set to test the positioning system including indoor and outdoor environments. Handset-side positioning mode and network-side positioning mode are provided simultaneously. Variety of motion models, such as static model, low-speed model and high-speed model are considered as well as different positioning algorithms. Finally, some implementation cases are analyzed to verify the credibility of the testbed.

Keywords: Fingerprint; WLAN; seamless positioning; testbed

This research is sponsored by the National Natural Science Foundation of China (No. 61401119), the National Science and Technology Major Project (No. 2015ZX03004002-004), the Distinguished Academic Leadership Foundation of Harbin (No. 2014RFXXJ002) and the Science and Technology Project of Ministry of Public Security, China，(No. 2015GABJC37).

http://dx.doi.org/10.3837/tiis.2016.06.008 **ISSN : 1976-7277**

1. Introduction

In recent years, location systems are growing rapidly. Global Navigation Satellite System (GNSS) is the the most effective positioning technology in terms of accuracy, availability and reliability in outdoor open environments [1]. However, the indoor positioning ability of GNSS is limited by insufficient satellite coverage [2]. There are many positioning technologies designed for indoor environments, such as Bluetooth positioning [3], Wireless Sensor Networks (WSN) positioning [4], Ultra Wideband (UWB) positioning [5], or some fusion techniques like hybrid RFID-WLAN positioning solutions [6]. Benefiting from the easy deployment and access [7], WLAN has been widely used for indoor positioning [8]. The location technologies based on WLAN mainly adopt Cell-Identification(Cell-ID), trilateration and fingerprint technique. While the accuracy of CELL-ID is too low to meet the requirement of the users, and the trilateration positioning process is affected by Non-Line-of-Sight (NLOS) greatly [9]. The most common approach for WLAN localization is fingerprint [10], and fingerprint positioning scheme is considered as the most promising technique for indoor positioning [11]. Fingerprint positioning contains two phases: off-line acquisition phase and on-line positioning phase [12]. During the off-line acquisition phase, received signal strength (RSS) is collected from the APs to build the radio map [13][14]. In the on-line positioning phase, the positioning results are calculated by comparing the gathered on-line RSS with the templates stored in the radio map.

Intuitively, software simulation is used to evaluate positioning techniques. However, software simulation is not always convincing and credible. To develop a practical system, taking actual experiments is necessary and testbed plays a more reliable role in evaluating positioning systems. In literatures [15][16][17][18][19], the positioning scenarios of testbeds are small scale and limited to floors in office buildings. The testbeds designed for testing WSN's in Steyn' paper [20] are not suitable for indoor localization. In literatures [21][22], the outdoor scenario is used for the fingerprint positioning, however, only the handset-side positioning mode is used in their experiments. Arya selected an outdoor area in Paris to be the testing scenario [23], but only static positioning model is considered in its positioning experiments. In this paper, we present a testbed evaluating fingerprint based WLAN positioning system. This proposed testbed can provide direct evaluation results indexed by accuracy of positioning. It is not only suitable for the small scale indoor scenario but also for the large scale indoor scenario and the outdoor scenario with sufficient WLAN signal coverage. The positioning mode of network-side positioning is also realized in this testbed besides the handset-side positioning mode. We consider three mobility models including static model, low-speed model and high-speed model in the testbed system. Different positioning algorithms such as K Nearest Neighbor (KNN), Weighted K Nearest Neighbors (WKNN) [24], Particle Filtering [25], Map Matching [26] and probabilistic approach [27] can be tested here. A joint and intelligent AP selection algorithm [28] and a novel group discriminant (GD)-based AP selection approach for improving location fingerprint [29] can be verified in the proposed testbed. The optimization method of building radio map is indicated as one of the key challenges in fingerprint [30]. A novel technique for human traffic based radio map updating is proposed in [31] and Igor Bisio presents a trainingless approach for building radio map in [32]. The verification of these two methods for fingerprint database training can be taken here. Literature [33] presents a hybrid solution that fuses measurements of smartphone sensors with

wireless signals which can be tested in this testbed. The testbed is developed to meet different kinds of fingerprint positioning testing requirements.

The remainder of this paper is organized as follows. Section 2 describes different application scenarios of the proposed testbed. The system implementing is described in Section 3. Some typical testing implementation cases are discussed in Section 4. Finally, conclusions are given in Section 5.

2. Testing scenarios

We select the following four testing scenarios in the testbed system including indoor office scenario, indoor corridor scenario, outdoor scenario and indoor open scenario. The purpose of selecting these scenarios is to cover different application environments of fingerprint positioning systems.

2.1 Indoor Office Scenario

Indoor office scenario is a classical indoor application scenario and it is the most common scenario for indoor positioning systems. As shown in **Fig. 1**, we select an area in an office building. There are several compartments containing room 1014 to 1018 in this office. The Service Set Identifier (SSID) of the APs is from AP1 to AP8. The area is over 200 square meters.

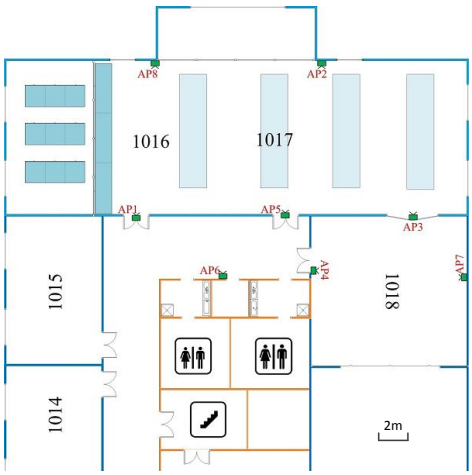

Fig. 1. Scenario **A**: Indoor office, with room from 1014 to 1018.

2.2 Indoor Corridor Scenario

The feature of indoor corridor scenario is narrow and long. Just as shown in **Fig. 2**, the gray shadow area in the figure is a corridor selected in an office building.

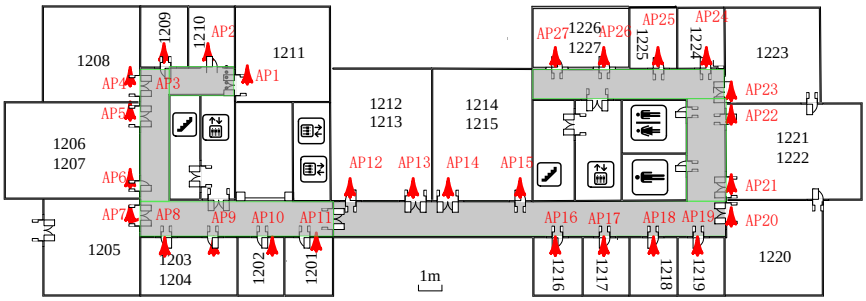

Fig. 2. Scenario **B**: Indoor corridor, with room from 1201 to 1227.

The APs are shown as arrows. The total number of the APs is 27, and the SSID is from AP1 to AP27. The area is about 1100 square meters. As the APs are deployed intensively about 3 meters with each other, it is able to take AP location optimization tests in this scenario. The distance between neighboring RPs (Reference Points) is 0.5 meter. We can take the tests on the different densities of the radio map in this scenario. The radio map is acquired by smartphones in indoor office scenario and laptops in indoor corridor scenario. The tests of different acquisition methods of radio map can be taken with the combination of these two scenarios.

2.3 Outdoor Scenario

Fingerprint positioning is usually used in indoor environments. In this paper, we extend fingerprint positioning environments to outdoor. As shown in **Fig. 3**, it is an outdoor scenario with the area of over 15000 square meters. The distance between neighboring RPs is 2 meters. There are totally up to 63 APs deployed in this scenario. And ten switches are deployed to keep smooth communication links.

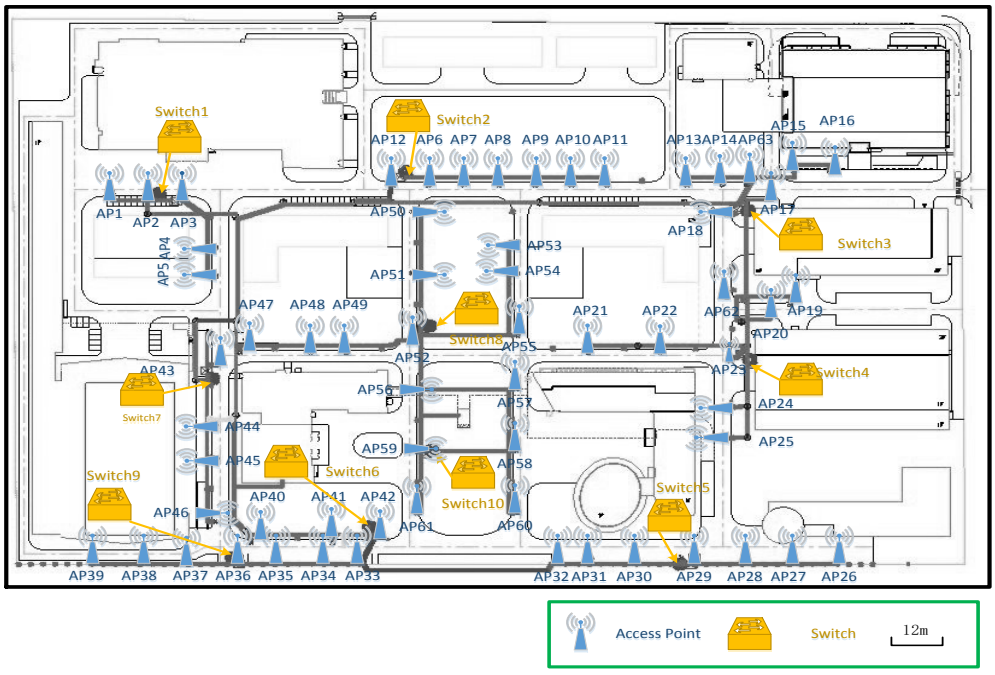

Fig. 3. Scenario **C**: Outdoor.

Lots of experiments can be taken in this scenario such as different mobility model tests, different positioning modes tests and so on. The experiment of data fusion is feasible in the narrow road between two high buildings where some positioning satellites are blocked. In this area, the positioning fusion of GNSS positioning and fingerprint positioning will provide us with better locating accuracy.

2.4 Indoor Open Scenario

An underground garage is selected as the indoor open scenario. It is a big open indoor environment with the area over 3000 square meters. The garage environment varies more greatly than other scenarios because of cars' driving in and out. The influence of different parking situations to the fingerprint positioning can be tested here.

As shown in **Fig. 4**, there are 27 APs and 3 switches in this scenario. The positioning mobility model is always static model in the former indoor positioning systems. The low-speed model can be tested in this scenario benefiting from the big open environment. As the arrows pointed, the passageways are the areas which connect the outdoor and the indoor. In literature [34], the author proposes a Euclidean distance based handoff algorithm for fingerprint positioning of WLAN system. The handoff algorithm can be verified in the passageway areas.

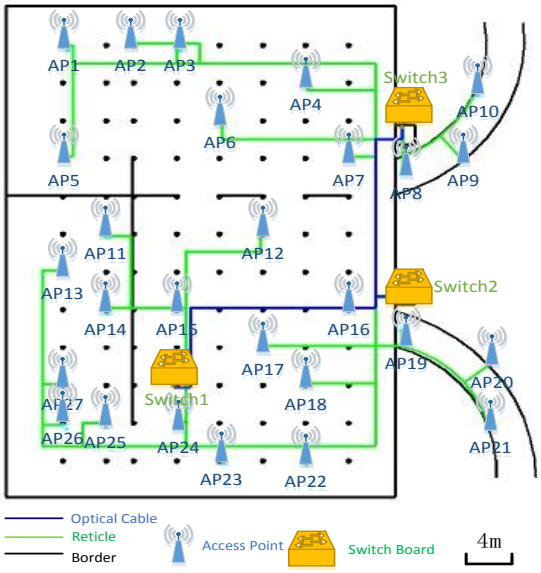

Fig. 4. Scenario D: Indoor open.

In the above four testing scenarios, we can realize a variety of experiments, such as different acquisition methods different densities of radio map experiment, different mobility model experiment, different positioning mode experiment, positioning fusion experiment, AP location optimization experiment, handoff algorithm verification experiment and so on.

3. Testbed implementing

3.1 Overall Framework

The testbed system consists of four parts, as shown in **Fig. 5**, including WLAN positioning server, WLAN positioning terminal, AP units and positioning accuracy analysis system. The server provides center positioning function and AP control function. The terminal provides handset-side positioning function and data acquisition function. The APs provide positioning RSS and data transmission function in the wireless network. The positioning accuracy analysis system provides the function of analyzing the positioning accuracy of the positioning system.

In the positioning process, the RSS which is collected by the terminal from the APs is sent to the server. The server sends the positioning result to the terminal through the wireless network which is made up of the APs and switches. The positioning accuracy analysis system gathers the positioning results from the terminal, the relative coordinates from the designated standard origin and the GNSS positioning result from the Real-Time Kinematic (RTK).

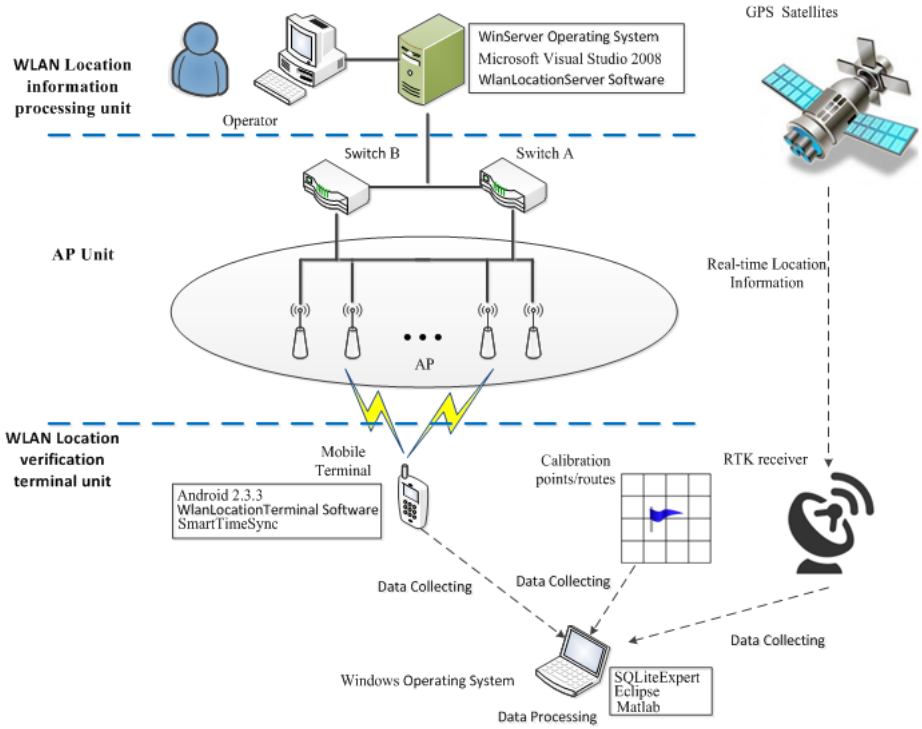

Fig. 5. Testbed architecture diagram.

3.2. The Positioning Server Implementing

3.2.1. Positioning Server Architecture

The workflow of positioning server is shown in **Fig. 6**. It indicates how the information flows in the system and what the server' working process is. There are three modules including AP controlling module, positioning algorithm module and transmission protocol module.

In AP controlling module, some status of APs can be controlled by the network center including AP' on-off, AP' transmission power and deployment. It is convenient to make testing on AP deployment with this module.

Positioning algorithm module, which is designed to achieve network-side positioning, can be used to test the performance of different positioning algorithms by replacing the existing algorithm with another one. At the same time, it can also provide monitoring function and positioning information fusion in the network center. For example, operators can monitor the mobile location in the network center when the mobile is installed on intelligence robot in the testing scenario. When other positioning methods such as bluetooth positioning, visual positioning are adopted in this testbed, the fusion of different positioning methods can be proceed in the network center. In transmission protocol module, the transmission protocol adopts TCP/UDP [35] at ordinary time. The MAC layer of AP is based on IEEE 802.11 MAC (CSMA/CA). Each of them radiates wireless signal in ISM 2.4GHz frequency band with transmission power of about 100mW and radiation radius is 100m.

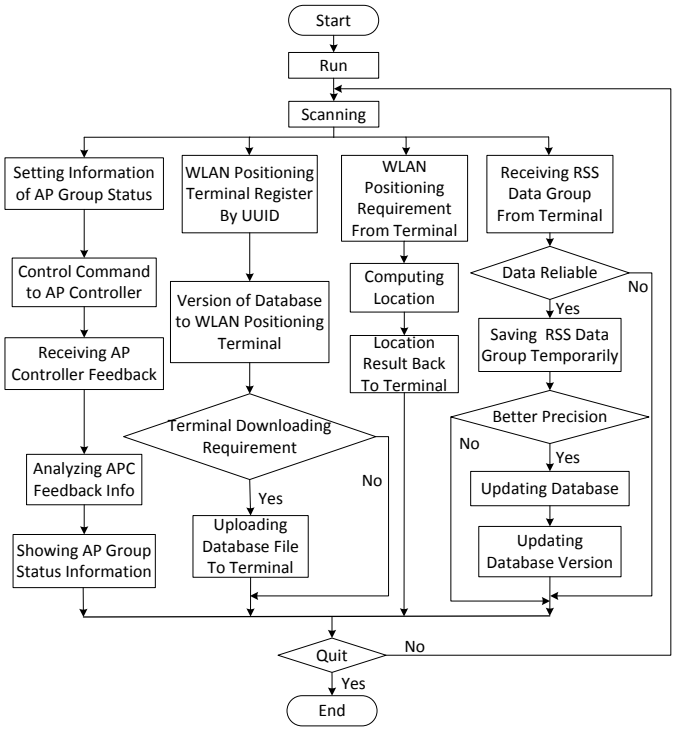

Fig. 6. Positioning server workflow diagram.

The positioning server configuration should be considered from both physical and application layer. Taking the underground garage scenario as an example, the elements of the physical and application layer of the positioning server are mainly in **Table 1**.

Table 1. Elements in physical and application layer of the testbed

Device Name	Device Type	Application
WLAN Positioning Server	WAVE NF8560M2	Positioning, Database updating, AP setting
WLAN Positioning Terminal	SAMSUNG I9250	RSS measurement, Data transportation
Access Point	CISCO AIR1242	CISCO AIR1242
Switch	HUAWEI SL7000	Connection between AP and AP controller
AP Controller	CISCO AIR-CT5508-100-K9	AP status controlling

3.2.2. Evaluation for Network Transmission

In the network-side positioning, a new problem which must be faced is network transmission. It is the link between server and terminal. One representative parameter to evaluate the performance of network transmission is Packet Loss Rate (PLR) [36].

PLR indicates the ratio of losing packets during packets transmission. At times, PLR is also considered as the frequency of packet loss event (PLE) which implies that there are one or more packets lost during one single round trip time (RTT) [37].

The transportation protocol module provides several fundamental algorithms to analyze PLR, such as single RTT packet sampling and single RTT time sampling. Packet sampling means that the computation of PLR is based on the statistic of the lost packets number and all the packets number. Time sampling is based on statistic of the packet loss period and the whole transmission period. Single RTT packet sampling is given by

$$P = \frac{N_{L0}^{'}}{N_0} \tag{1}$$

where P stands for packet loss rate, $N_{L0}^{'}$ stands for quantity of losing packets in a single RTT, N_0 stands for quantity of total packets in a single RTT.

It works efficiently because of the low complexity of the algorithm. However, it is not applicable when RTT changes rapidly. Single RTT time sampling is given by

$$P = \frac{T_{L0}^{'}}{T_0} \tag{2}$$

where $T_{L0}^{'}$ stands for the period of packet loss time (PLT), T_0 stands for the period of RTT.

This method is nearly the same as single RTT packet sampling except that it depends on time statistic. On account to the contingency by using only one RTT, PLR will be affected heavily by changes of RTTs. We propose Multiple RTT algorithm to make the estimation of PLR more suitable to the statistical rule. Multiple RTT packet sampling is given by

$$P = \frac{\sum_{i=0}^{n} P_i}{n} = \frac{\sum_{i=0}^{n} \frac{N_{Li}^{'}}{N_i}}{n} \tag{3}$$

where P_i stands for packet loss rate of i_{th} RTT, n stands for the quantity of RTT, $N_{Li}^{'}$ stands for the quantity of losing packets in i_{th} RTT, N_i stands for the quantity of total packets in i_{th} RTT.

This method performs better than single RTT when each RTT changes rapidly when using a group of RTTs, while during each RTT quantities of total packets should be stable. Multiple RTT time sampling is given by

$$P = \frac{\sum_{i=0}^{n} P_i}{n} = \frac{\sum_{i=0}^{n} \frac{T_{Li}^{'}}{T_i}}{n} \tag{4}$$

where T_i stands for period of PLT in i_{th} RTT, $T_{Li}^{'}$ stands for period in i_{th} RTT.

For eliminating the effect of difference of each RTT completely, we propose packet-weighted and time-weighted algorithm as the improved algorithm. Packet-weight indicates the weight of each RTT is which achieved by the ratio of the losing packets number

to totally-transmitted ones, while time-weight indicates the weight of both periods.Packet -weighted multiple RTT time sampling is given by

$$P = \frac{\sum_{i=0}^{n} N_i \times P_i}{\sum_{i=0}^{n} N_i} = \frac{\sum_{i=0}^{n} N_i \times \frac{T_{Li}^{'}}{T_i}}{\sum_{i=0}^{n} N_i} \tag{5}$$

In this method, P_i is weighed by the ratio of different N_i to avoid being affected by changes of number of packets during each RTT. Time-weighted multiple RTT packet sampling is given by

$$P = \frac{\sum_{i=0}^{n} T_i \times P_i}{\sum_{i=0}^{n} T_i} = \frac{\sum_{i=0}^{n} T_i \times \frac{N_{Li}^{'}}{N_i}}{\sum_{i=0}^{n} T_i} \tag{6}$$

In this method, P_i is weighed by the ratio of different T_i to avoid being affected by changes of period of RTTs. In terms of algorithms mentioned above, parameters like $N_{L0}^{'}, N_0, T_{L0}^{'}, T_0, N_{Li}^{'}, N_i, T_{Li}^{'}, T_i$ are available by using Wireshark, a capturing packet software.

We take a test of PLR with a total sampling time of 40 minutes using the last algorithm. An experimenter equipped with a mobile phone walks around the outdoor scenario. UDP is adopted as the transmission protocal. RTT fluctuates from 90 milliseconds to 150 milliseconds but arises to nearly 1 second sometimes. There are 2000 total packets transmitted during the test, while 76 packets are lost in the network transmission. And the calculated PLR is 3.8%.

There are two reasons of PLR. One is the switchover among different APs which give the path of fingerprint information and it is caused by the actual AP' deployment and AP' connection mechanism. The other one is network delay. The network delay implies the time interval between packet message entering and leaving the Ethernet. In terms of estimating network delay, some factors should be considered.

$$T = T_{up} + T_{down} = T_c + T_j + \Delta t \tag{7}$$

where T stands for total network delay, T_{up} stands for uplink time delay, T_{down} stands for downlink time delay, T_c stands for time delay caused by network congestion, T_j stands for time delay by network jitter, and Δt stands for time delay by other factors.

3.3. The Positioning Terminal Implementing

The proposal implementation over Android operating system-based terminal has been extensively tested [38]. In this testbed, an Android-based positioning terminal is designed. The Android system supports to access most mobile sensors. Benefitting from its good versatility, Android has been used in lots of mobile phones produced by different manufacturers such as HTC, Samsung, Motorola and so on. It is convenient to test the performance comparison in fingerprint-based indoor positioning system over different terminals [39].

As shown in **Fig. 7**, the terminal is made up of positioning module, time synchronization module and data recording module. The positioning module achieves location results by passing parameters to the positioning algorithm module. The parameter is collected by calling various sensors and the built-in WLAN scanning function of the android. The main purpose of

time synchronization is to facilitate positioning accuracy analysis and data fusion. The data recording module is used for the positioning accuracy analysis.

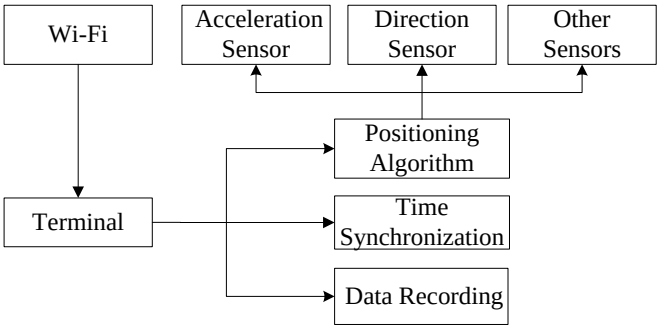

Fig. 7. Terminal structure diagram.

In the positioning module, four sensors are selected to be used in handset-side positioning including Acceleration Sensor, Direction Sensor, Gyro Sensor and Gravity Senor. These sensors offer the ability to physically measure the motion dynamics information, including the distance moved and the direction. The inertial navigation can be achieved by using these sensors. In this implementation, three directions of the terminal are defined as xyz, just as **Fig. 8** shows.

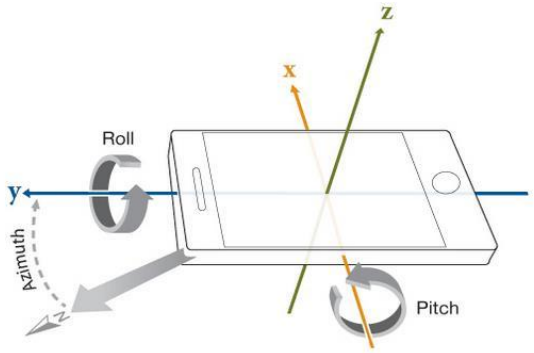

Fig. 8. Mobile phone axial diagram.

In the testbed, we consider different motion models including static model and dynamic model. A positioning fusion method between WLAN location and inertial navigation is presented in [40]. As the inertial navigation is practicable only when the terminal is dynamic, we need to know the motion models when the fusion method is tested. Literature [41] also proposes a model-based dynamic filter algorithm using an accurate model of mobile terminal motion. We can see that the motion model is important in terminal positioning. Here, a judgment method is designed to distinguish the terminal's motion state.

The Euclidean distance [34] of adjacent two acceleration vector is considered to be the variable of judgment. A set of measuring acceleration values are measured every 200 milliseconds. Assuming that the acceleration value is $X_n Y_n Z_n$ in time n, $X_{n-1} Y_{n-1} Z_{n-1}$ in time $n-1$. Let *StageFlag* stands for the motion state of the terminal, *acc* stands for the European distance. They are given by

$$\begin{cases} acc = \sqrt{w_1 \times (X_n - X_{n-1})^2 + w_2 \times (Y_n - Y_{n-1})^2 + w_3 \times (Z_n - Z_{n-1})^2} \\ stageFlag = 0 \quad acc < \varepsilon \\ stageFlag = 1 \quad acc \geq \varepsilon \end{cases} \tag{8}$$

where w_1, w_2, w_3 stand for the weight of every direction, and they need to meet $w_1 + w_2 + w_3 = 1$, ε stands for the threshold value which is set according to different situations. $stageFlag = 0$ stands for the terminal is static and $stageFlag = 1$ stands for the terminal is moving.

In the time synchronization module, there are two methods such as GPS (Global Position System) synchronization and NTP (Network Time Protocol) synchronization. GPS synchronization will be mentioned in later sections. As shown in **Fig. 9**, the fundamental of NTP synchronization is as follows.

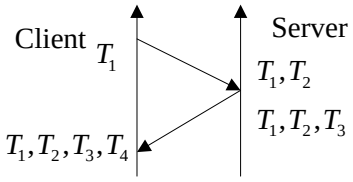

Fig. 9. NTP time synchronization principle diagram.

Firstly, the terminal sends a NTP packet with a timestamp T_1 to the network server, and the time of the server receiving the packet is T_2. Then, the server sends a new packet to the terminal with a new timestamp T_3, and the time of the terminal receiving the new packet is T_4. We need two important parameters to get the time synchronization. They are given by

$$\begin{cases} Delay = (T_4 - T_1) - (T_3 \_ T_2) \\ Offset = \dfrac{1}{2} \times [(T_2 - T_1) + (T_3 - T_4)] \end{cases} \tag{9}$$

where *Delay* stands the time delay of a transmission cycle, *Offset* stands for the time difference of the terminal and the server.

In the data recording module, we need to provide height compensation because of the references and the terminal are in different height. Take the outdoor scenario in Section 2 as an example. World Geodetic System-1984 Coordinate System (WGS84) is selected to be reference frame in this scenario. It is needed to take a coordinate transformation between WGS84 and Earth Centered Earth Fixed (ECEF) to realize height compensation. Firstly, we need to transform the WGS84 to ECEF [42]. They are given by

$$\begin{cases} b = \arctan \dfrac{z \times (N+h)}{\sqrt{(x^2+y^2)} \times (N \times (1-e^2)+h)} \\ l = \arctan(\dfrac{y}{x}) \\ h = \dfrac{\sqrt{(x^2+y^2)}}{\cos b} - N \end{cases} \tag{10}$$

where xyz stand for the coordinates in WGS84, and blh stand for the coordinates in ECEF. N stands for the earth's surface prime vertical curvature radius. e stands for the first eccentricity of the earth.

Then we take the height compensation given by

$$h' = h + \Delta h \tag{11}$$

where h' stands for the height compensated, Δh stands for height compensating factor.

At last, the ECEF is transformed back to WGS84 which is given by

$$\begin{cases} x = (N+h') \times \cos b \times \cos l \\ y = (N+h') \times \cos b \times \sin l \\ z = [N \times (1-e^2)+h'] \times \sin b \end{cases} \tag{12}$$

3.4. Positioning accuracy analysis system

Positioning accuracy analysis system is one of the most important parts in testbeds. Here, we providedifferentkindsofpositionreferencesfordifferenttestenvironmentsincludingCalibrationpoints, Calibration routes and Real - Time Kinematic (RTK) receiver.

3.4.1. Calibration points

Calibration points are used in indoor static positioning experiments. Some points are demarcated in the indoor environments as calibration points, the coordinates of the calibration points can be measured exactly, according to the coordinate system of the scenarios.

In some scenarios, such as the underground garage, the reference points can be obtained from outdoors by the passageway by using professional mapping instruments. Then the absolute coordinates (global coordinate) will be taken. However, in some other scenarios, such as typical office building, we can only take the relative coordinate (local coordinate) as calibration. The calibration points' coordinates can be measured according to the position relationship among the RPs.

3.4.2. RTK receiver

RTK receiver is the obvious choice for outdoor position reference. There are 3 problems in practical using: synchronization problem; accuracy problem and antenna position compensation problem.

To solve the GPS time synchronization [43] problem, the GPS weak number (WN) and the GPS time of week (TOW) are recorded by the RTK receiver. The UTC (Coordinated Universal Time) time is also recorded by the WLAN positioning equipment. As the data refresh rate of WLAN positioning equipment is much slower than the RTK receiver's, the time scales of WLAN positioning results are used as benchmarks, the temporally closest RTK

positioning result will be selected as the corresponding position reference. The synchronization judgment condition is illustrated as follows.

$$T_{RTK} = \frac{T_{UTC}}{1000} - WN \times 7 \times 24 \times 3600 - TOW - 3657 \times 24 \times 3600 + N - 19 \quad (13)$$

where T_{RTK} indicates the data refresh cycle. T_{UTC} stands for the UTC time recorded by the WLAN positioning equipment in milliseconds. N indicates the leap seconds which is announced by International Earth Rotation Service (IERS), for example in December 2005 $N = 32$, in January 2006 $N = 33$.

The last problem is antenna position compensation. The positioning results provided by the WLAN positioning equipment and the RTK receiver are supposed to be the positions of their antennas. But one antenna cannot overlap the other one. This brings the antenna position compensation problem.

As the orientation of the experimental platform is randomized, the antenna position cannot be compensated easily in the absolute coordinates. In this testbed, the two antennas are placed along the axis of the travel direction, thus the direction of the antenna compensation can be replaced by travel direction, as shown in **Fig.10**.

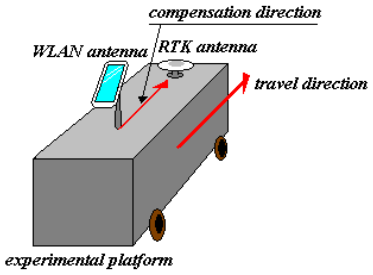

Fig. 10. Experimental platform diagram.

The travel direction can be calculated by 2 RTK positioning results, which is shown by

$$V_{travel} = (X_{t-\Delta t} - X_{t+\Delta t}, Y_{t-\Delta t} - Y_{t+\Delta t}, Z_{t-\Delta t} - Z_{t+\Delta t}) \quad (14)$$

where vector V_{travel} reflects the travel direction, (X_t, Y_t, Z_t) means the selected RTK position reference; $(X_{t-\Delta t}, Y_{t-\Delta t}, Z_{t-\Delta t})$ and $(X_{t+\Delta t}, Y_{t+\Delta t}, Z_{t+\Delta t})$ indicate 2 RTK positioning results, Δt is the interval time.

Supposing that the distance between two antennas is d_{ant}, the compensation vector V_{comp} is calculated as follow.

$$V_{comp} = \frac{d_{ant} \times V_{travel}}{|V_{travel}|} \quad (15)$$

In the proposed testbed, $d_{ant} = 0.3m$ is used for low-speed platform, $d_{ant} = 1m$ is used for high-speed platform. Supposing that the WLAN positioning result is indicated by vector R_{temp}, the compensated position can be indicated by vector $R_{comp} = R_{temp} + V_{comp}$. The positioning error is calculated by R_{comp} and corresponding RTK position.

3.4.3. Calibration routes

Calibration routes are used in indoor-low speed positioning experiments. When the receiver is moving in indoor environments, the synchronized position reference is absent. To solve this problem, calibration routes are introduced in the testbed system. In both absolute coordinates and relative coordinate systems, two calibration points can determine a straight line as shown in Equation 16.

$$\frac{X - X_A}{X_B - X_A} = \frac{Y - Y_A}{Y_B - Y_A} = \frac{Z - Z_A}{Z_B - Z_A} \tag{16}$$

where (X_A, Y_A, Z_A) and (X_B, Y_B, Z_B) indicate the coordinates of calibration point A and B.

If the user is moving along the calibration route, the perpendicular distance between the positioning result and the calibration route can be calculated, as shown by D_1, D_2, D_3, D_4, D_5 in **Fig. 11**.

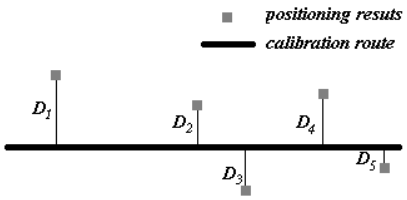

Fig. 11. Perpendicular distance diagram.

In our fingerprint systems, terminals move in a common plane, so the height of the mobile is considered to be constant. So the 3D question is changed to be a 2D one. Statistically, the real positioning error E can be obtained by the perpendicular distance D after compensation, as shown in **Fig. 12.**

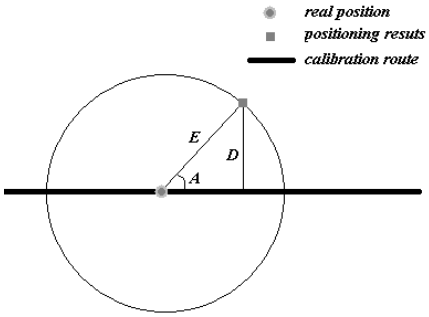

Fig. 12. Compensation method diagram.

Due to the randomness of the error, the angle deviation A can be considered uniformly distributed. The statistical relationship between E and D can be calculated by Equation 17.

$$E = \int_0^{2\pi} |D \arcsin(A)| dA = \sqrt{2} D \tag{17}$$

The value of vertical distance is calculated by Equation 18.

$$\begin{cases} D_i = \dfrac{|V_{AB} \times V_i|}{V_{AB}} \\ V_{AB} = (X_A - X_B, Y_A - Y_B, Z_A - Z_B) \\ V_i = (X_A - X_i, Y_A - Y_i, Z_A - Z_i) \end{cases} \tag{18}$$

where D_i indicates the perpendicular distance between the i_{th} positioning result and the calibration route. (X_i, Y_i, Z_i) indicates the coordinates of the i_{th} positioning result.

Thus, during the indoor low speed positioning experiments, the receiver should move along the calibration route, and record the positioning results. During the accuracy analysis process, the perpendicular distance between the positioning results and the calibration route is calculated. The statistical value of D is obtained by Equation 19.

$$E_{mean} = \sqrt{2} D_{mean} \tag{19}$$

where E_{mean} and D_{mean} indicate the mean values of E and D respectively.

As mentioned, the absolute coordinates is used in the underground garage scenario, so the calibration routes and calibration points cannot be selected freely. **Fig. 13** demonstrates the distribution of the calibration routes and calibration points. The white points stand for the calibration points and the white lines stand for calibration routes.

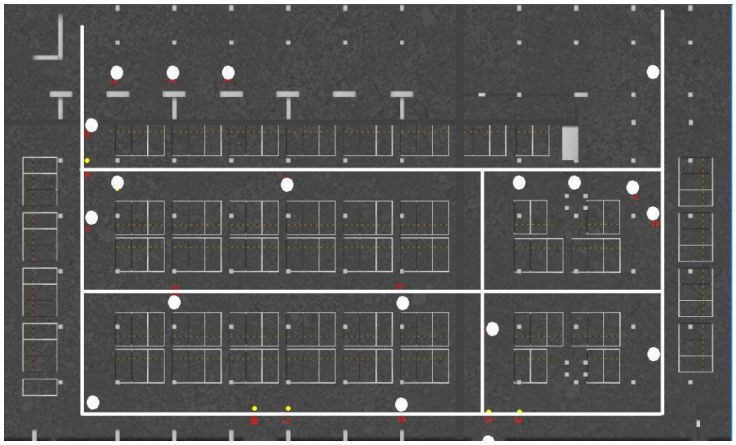

Fig. 13. Calibration routes and points diagram.

4. Implementation cases

There are many positioning cases which can be implemented in different scenarios in the testbed system. Here, we just put forward several examples.

The offline phase is an essential part of the fingerprint. Here, we take the method as followed. Equally spaced RPs are selected to build the radio map. At each RP, we choose four orthogonal directions and 100 RSS samples are gathered for every direction. Then the mean value of RSS in all 100 samples is considered as the fingerprint at this direction of the RP. All the fingerprints form the radio map. For example, by taking this method, we got 414 RPs in indoor corridor scenario and 6629 RPs in outdoor scenario.

Firstly, we take a test about the grid size of radio map in Scenario A. The gird size reflects

the dense of radio map and it is a significant impact factor in fingerprint positioning. Taking 0.5 meter as a step, the grid size of radio map is set ranging from 0.5m to 2m. At the same time, noises with different variance are drawn in to demonstrate different qualities of radio map. As shown in **Fig. 14**, X axis presents the variance of the noise and Y axis stands for the mean positioning accuracy. It can be seen that the positioning accuracy is influenced by grid size. With the same radio map quality, a smaller grid size lead to a better positioning accuracy.

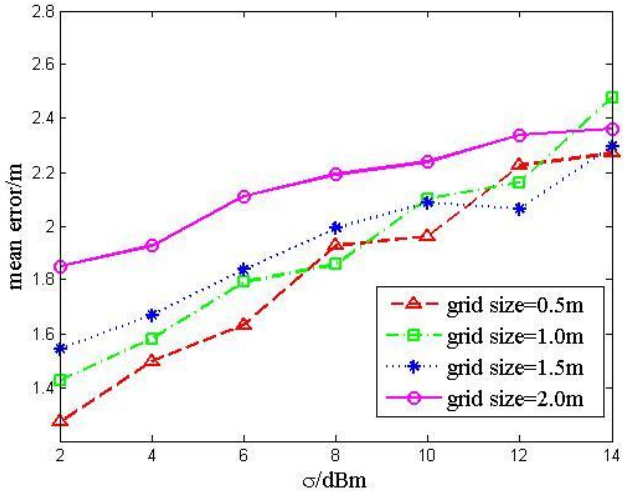

Fig. 14. Experiment of different grid sizes.

Then, a RSSI sample number test is carried on also in Scenario A. During the online phase, there may be different RSSI sample numbers that can be used in a single positioning process. For example, if the refresh frequency of beacon frame is 10Hz and the location result is provided per second, there will be 10 RSSI sample numbers that can be adopted. The same to the above test, the radio map is also appended with noises and the grid size is set to be 0.5m. As **Fig. 15** shows, 10, 50 and 100 samples are selected respectively in the test. Basically, larger sample numbers correspond to better positioning accuracy.

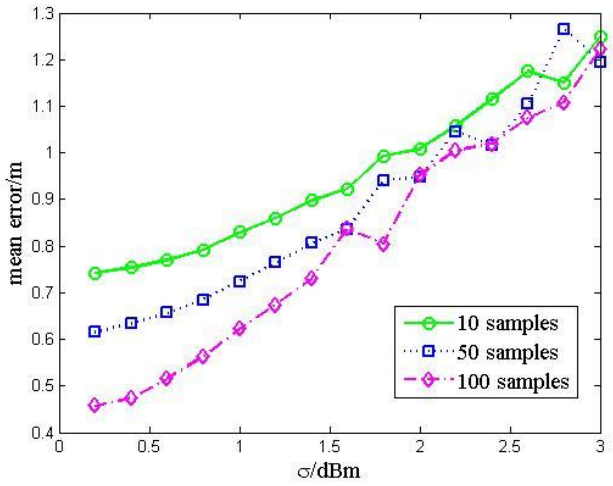

Fig. 15. Experiment of different RSSI sample numbers.

A test of autonomous radio map acquisition is shown in **Fig. 16**. As there is much workload in the radio map acquisition process, some scholars proposed the autonomous radio map acquisition technique. In the autonomous acquisition, people just need to take one or several normal walking measurements to build up the radio map rather than stand for a long time in every reference point. In Scenario B, we take this test in the office corridor in which the mean errors are compared between different times of walking measurements. From the figure, we can see that the trend of the positioning accuracy becomes better when the times of walking measurements increase.

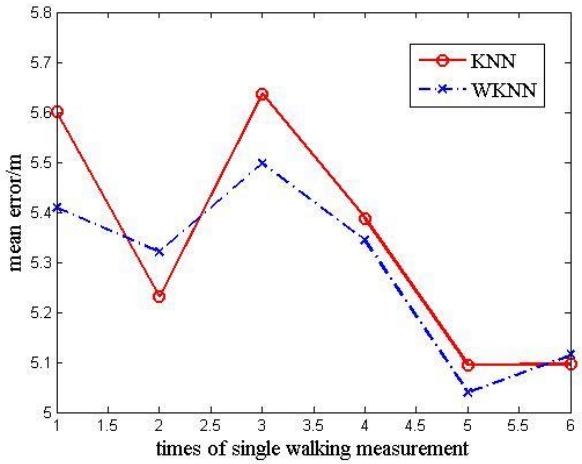

Fig. 16. Experiment of autonomous radio map acquisition.

We take an experiment of different AP numbers in Scenario C. As shown in **Fig. 17**, the two curves stand for different positioning performance with 63 APs and 40 APs. The 40 APs are selected from the 63 APs. In a general way, if there are more APs, the positioning will be more precise. From the Cumulative Distribution Function (CDF) of positioning error, we can get that the test's result conforms to this rule on the whole.

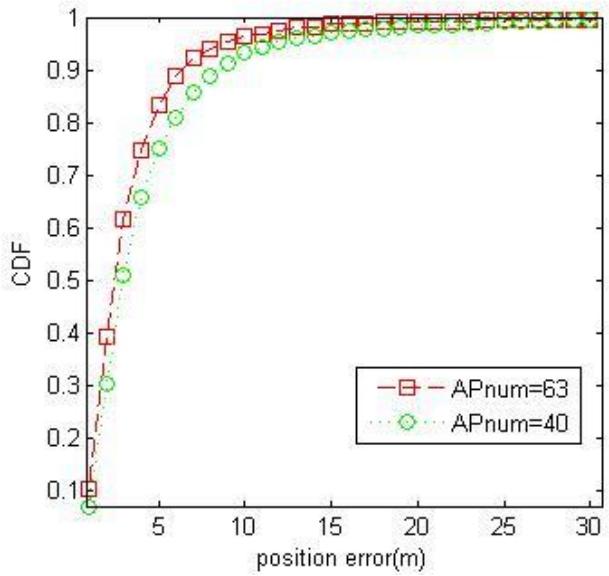

Fig. 17. CDF of positioning error with different AP numbers.

Fig. 18 shows an experiment of low-speed model and high speed model in the outdoor environment in Scenario C. Different from general small indoor fingerprint positioning area, benefitting from the immense space in the Scenario C, we can test a high-speed 20m/s by a car's driving. And the low-speed is set to be 1m/s by a person' walking. RTK positioning results are taken as the position reference. We can get the accurate results of the two mobility models by comparing the mobile positioning results with the RTK positioning results. As we know, due to the time delay of the positioning algorithm, the positioning accuracy of low-speed model will be much better than the high-speed model. Here, a quantitative result is provided. Taking the position error 10m as an example, the CDF is about 60% in the high-speed model, while in the low-speed model the CDF reaches nearly 95%.

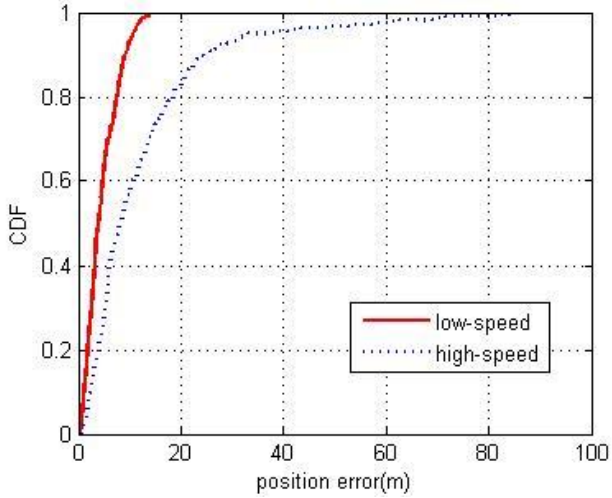

Fig. 18. CDF of positioning error of different speed model.

As shown in **Fig. 19**, we take a static model positioning test in three different testing Scenarios A, C and D. We take 2144 test points (TPs) in the indoor corridor, 1172 TPs in the outdoor scenario and 3383 TPs in the underground garage. In this test, we take the calibration points as the position reference. In the three different positioning scenarios, we adopt the same test factors such as radio map dense, RSSI sample numbers, positioning algorithm and so on except the AP deployment and actual physical environment. From the figure, we can see that the positioning accuracy of corridor is the best benefitting from the steady indoor environment. While in garage, the APs are deployed more dispersedly because of complex construction, and the fluctuation of RSS is huge on account of vehicles' driving frequently in and out. These disadvantageous factors lead to the worst accuracy in this scenario. Taking position error equals to 5m as an example, the CDF of Scenario D is about 60%, and in the Scenario C and B, it is nearly 80% and 100%, respectively. We can see that although using the same positioning algorithm, the positioning accuracy changes enormously between different scenarios. It is one of the key points that we propose the testbed to see the influence of different environments on fingerprint positioning technique.

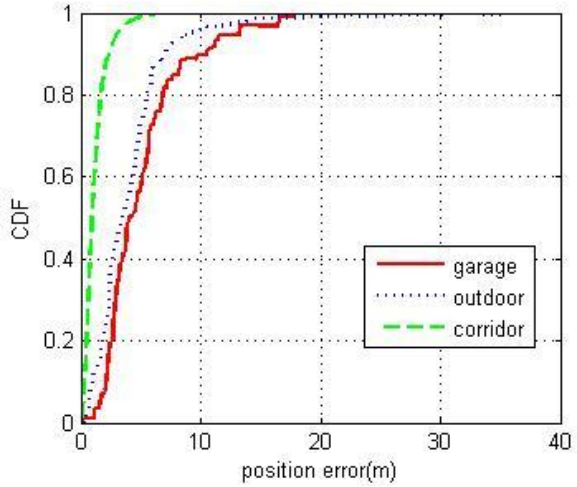

Fig. 19. CDF of positioning error of static mode test in different three scenarios.

There are a variety of experiments related to fingerpring positioning can be taken in the proposed testbed. The above six are just several conducted examples to present the universality of the testbed. Based on this testbed, we can carry on different experiments to verify most of the techniques in the fingerprint positioning systems.

5. Conclusion

A testbed of performance evaluation for fingerprint based WLAN positioning system is designed and tested. For realizing a whole testbed to testing the fingerprint position system, the positioning server, the positioning terminal and the positioning accuracy system are implemented. Disparate from other related testbeds which always focus on single test scenario, the proposed testbed cover both indoor and outdoor environment. Besides typical office scenario, the open underground garage with a large area is also tested. On account of the abundant scenarios, lots of experiments related to fingerprint positioning technique can be taken on. Through analyzing some implementation cases, it can be seen that the testbed has the possibility to proceed extensive reproducible experiments. It is such a comprehensive platform for positioning system that can be conducive to the further development of the fingerprint technology. In the future, the testbed can be promoted to contain more complex scenarios such as urban streets or fire scenes. To improve the robustness and reliability, there should be more experiments about algorithms or techniques related to fingerprint positioning.

References

[1] Kim M.; Seo J., Lee J. A Comprehensive Method for GNSS Data Quality Determination to Improve Ionospheric Data Analysis. *Sensor*, 14(8), 14971-14993, 2014. Article (CrossRef Link)

[2] Mo Y., Zhang Z., Meng W., Ma L. and Wang Y., "A Spatial Division Clustering Method and Low Dimensional Feature Extraction Technique Based Indoor Positioning System," *Sensors*, vol. 14, no. 1, pp. 1850-1876, 2014. Article (CrossRef Link)

[3] Zhou S., Pollard and J. K., "Position measurement using Bluetooth," *Consumer Electronics, IEEE Transactions on*, vol. 52, no. 2 pp. 555-558, May, 2006. Article (CrossRef Link)

[4] Han Guangjie, et al., "The Insights of Localization through Mobile Anchor Nodes in Wireless Sensor Networks with Irregular Radio," *Ksii Transactions on Internet & Information Systems*, vol. 6, no. 11, pp. 2992-3007, November 2012. Article (CrossRef Link)
[5] Mahfouz M. R, et al. "Investigation of High-Accuracy Indoor 3-D Positioning Using UWB Technology," *Microwave Theory and Techniques, IEEE Transactions on*, vol. 56, no. 6, pp. 1316-1330, June 2008. Article (CrossRef Link)
[6] Lohan E S, Koski K, Talvitie J, et al., "WLAN and RFID Propagation channels for hybrid indoor positioning," in *Proc. of Localization and GNSS (ICL-GNSS), 2014 International Conference on. IEEE*, pp 1-6, June 24-26, 2014. Article (CrossRef Link)
[7] Rubino I., Xhembulla J., Martina A., Bottino, A. and Malnati, G., "MusA: Using Indoor Positioning and Navigation to Enhance Cultural Experiences in a Museum," *Sensors*, vol. 13, pp. 17445-17471, 2013. Article (CrossRef Link)
[8] Talvitie J., Renfors M. and Lohan, E.S., "Distance-Based Interpolation and Extrapolation Methods for RSS-Based Localization With Indoor Wireless Signals," *Vehicular Technology, IEEE Transactions on*, vol. 64, no. 4, pp. 1340-1353 April, 2015. Article (CrossRef Link)
[9] Peng M, Zhou Q F, Cheng X. "NLOS aware TOF positioning in WLAN," in *Proc. of Wireless Communications & Signal Processing (WCSP), 2015 International Conference on. IEEE*, pp. 1-5, Oct. 15-17, 2015. Article (CrossRef Link)
[10] Collotta M, Lo Cascio A, Pau G, et al., "Smart localization platform for IEEE 802.11 industrial networks," in *Proc. of Industrial Embedded Systems (SIES), 2013 8th IEEE International Symposium on. IEEE*, pp.69-72, June 19-21, 2013. Article (CrossRef Link)
[11] Deyue Zou, Weixiao Meng, Shuai Han, Zijun Gong and Baoguo Yu. "User Aided Self-growing Approach on Radio Map Construction for WLAN based Localization," in *Proc. of 26th International Technical Meeting of the Satellite Division of the Institute of Navigation*, pp. 991-997, September 16-29, 2013. Article (CrossRef Link)
[12] Igor Bisio, Fabio Lavagetto, Mario Marchese, Andrea Sciarrone, "Energy Efficient WiFi-based Fingerprinting for Indoor Positioning with Smartphones," in *Proc. of IEEE Global Communications Conference*, pp. 4639-4643 Dec. 2013. Article (CrossRef Link)
[13] Bshara, M., Orguner, U., Gustafsson, F., Van Biesen, L., "Fingerprinting Localization in Wireless Networks Based on Received-Signal-Strength Measurements: A Case Study on WiMAX Networks," *Vehicular Technology, IEEE Transactions on*, vol. 59, no. 1, pp. 283-294, 2010. Article (CrossRef Link)
[14] C. Feng, W. Au, S. Valaee, Z. Tan, "Received-signal-strength-based indoor positioning using compressive sensing," *Mobile Computing, IEEE Transactions on* vol. 11, no.12, pp. 1983-1993, 2012. Article (CrossRef Link)
[15] Shih-Hau Fang, Chu-Hsuan Wang, "A Dynamic Hybrid Projection Approach for Improved Wi-Fi Location Fingerprinting," *Vehicular Technology, IEEE Transactions on*, vol. 60, no. 3, pp. 1037-1044, 2011. Article (CrossRef Link)
[16] Adler S, Schmitt S, Will H, et al. "Virtual Testbed for Indoor Localization," in *Proc. of Indoor Positioning and Indoor Navigation (IPIN), 2013 International Conference on. IEEE*, pp. 1-8, Oct. 28-31, 2013. Article (CrossRef Link)
[17] Zhao, Z., Yang, G.-H., Liu, Q., Li, V.O.K., Cui, L., "Implementation and application of a multi-radio wireless sensor networks testbed," *Wireless Sensor Systems, IET*, vol. 1, no. 4, pp. 191-199. December, 2010. Article (CrossRef Link)
[18] Nafarieh A. and Ilow J., "A Testbed for Localizing Wireless LAN Devices Using Received Signal Strength," in *Proc. of Communication Networks and Services Research, Annual Conference on IEEE*, pp.481-487, May 5-8, 2008. Article (CrossRef Link)
[19] Jan, S.-S., Hsu, L.-T., Tsai, W.-M., "Development of an Indoor Location Based Service Test Bed and Geographic Information System with a Wireless Sensor Network," *Sensors*, vol. 10, no. 4, pp. 2957-2974, 2010. Article (CrossRef Link)
[20] Steyn, L. P., Hancke, G.P., "A survey of Wireless Sensor Network testbeds," in *Proc. of AFRICON, 2011, IEEE*, pp.1-6, Sept. 13-15, 2011. Article (CrossRef Link)

[21] Qingyuan Zhao, Sheng Zhang, Xingchuan Liu, Xiaokang Lin, "An effective preprocessing Scheme for WLAN-based fingerprint positioning systems," in *Proc. of Communication Technology (ICCT), 2010 12th IEEE International Conference on IEEE*, pp. 592-595, Nov. 11-14 2010. Article (CrossRef Link)
[22] Xing-chuan Liu, Sheng Zhang, Heng-hui Lu, Xiao-kang Lin, "Method for efficiently constructing and updating radio map of fingerprint positioning," in *Proc. of GLOBECOM Workshops (GC Wkshps), 2010 IEEE*, pp. 74-78, Dec. 6-10, 2010. Article (CrossRef Link)
[23] Arya, A, Godlewski, P., Campedel, M., du Chene, G., "Radio Database Compression for Accurate Energy-Efficient Localization in Fingerprinting Systems," *Knowledge and Data Engineering, IEEE Transactions on*, vol. 25, no. 6, pp. 1368-1379, 2013. Article (CrossRef Link)
[24] Hsu, L-T., Tsai, W-M., Jan, S-S., "Development of a Real Time Indoor Location Based Service Test Bed," in *Proc. of Proceedings of ION GNSS*, pp. 1175-1183, September, 2010. Article (CrossRef Link)
[25] Georgy J., Noureldin A. and Goodall, C., "Vehicle navigator using a mixture particle filter for inertial sensors/odometer/map data/GPS integration," *Consumer Electronics, IEEE Transactions on*, vol. 58, no. 2, pp. 544-552, 2012. Article (CrossRef Link)
[26] Zampella F., Jimenez Ruiz, A.R. and Seco F., "Indoor Positioning Using Efficient Map Matching, RSS Measurements, and an Improved Motion Model," *Vehicular Technology, IEEE Transactions on*, vol. 64, no. 4, pp. 1304-1317, 2015. Article (CrossRef Link)
[27] Moghtadaiee V. and Dempster A.G., "Indoor Location Fingerprinting Using FM Radio Signals," *Broadcasting, IEEE Transactions on*, vol. 60, no. 2, pp. 336-346, 2014. Article (CrossRef Link)
[28] Deng Z A, Xu Y B, Ma L. "Joint Access Point Selection and Local Discriminant Embedding for Energy Efficient and Accurate Wi-Fi Positioning," *Ksii Transactions on Internet & Information Systems*, vol. 6, no. 3, pp. 794-814, 2012. Article (CrossRef Link)
[29] Lin T. N., Fang S. H., Tseng W. H., Lee C. W. and Hsieh, J. W., "A group-discrimination-based access point selection for WLAN fingerprinting localization," *Vehicular Technology, IEEE Transactions on*, vol. 63, no. 8, pp. 3967-3976, 2014. Article (CrossRef Link)
[30] Sorour S., Lostanlen Y., Valaee S. and Majeed, K., "Joint Indoor Localization and Radio Map Construction with Limited Deployment Load," *Mobile Computing, IEEE Transactions on*, vol. 14, pp. 1031-1043, 2015. Article (CrossRef Link)
[31] Mo Y, Zhang Z, Lu Y, et al. "A novel technique for human traffic based radio map updating in Wi-Fi indoor positioning systems," *Ksii Transactions on Internet & Information Systems*, vol. 9, no. 5, pp. 1881-1903, 2015. Article (CrossRef Link)
[32] Igor Bisio, Matteo Cerruti, Fabio Lavagetto, Mario Marchese, Matteo Pastorino, Andrea Randazzo and Andrea Sciarrone, "A Trainingless WiFi Fingerprint Positioning Approach over Mobile Devices," *IEEE Antennas and Wireless Propagation Letters*, vol. 13, no. 1, pp. 832-835, 2014. Article (CrossRef Link)
[33] Liu J., Chen R., Pei L., Guinness R. and Kuusniemi H., "A Hybrid Smartphone Indoor Positioning Solution for Mobile LBS," *Sensors*, vol. 12, no. 12, pp. 17208-17233, 2012. Article (CrossRef Link)
[34] Deyue Zou, Weixiao Meng and Shuai Han, "Euclidean distance based handoff algorithm for fingerprint positioning of WLAN system," in *Proc. of Wireless Communications and Networking Conference*, pp. 1564-1568, April 7-10, 2013. Article (CrossRef Link)
[35] Hwangnam Kim and Jennifer C. Hou, "Improving protocol capacity for UDP/TCP traffic with model-based frame scheduling in IEEE 802.11-operated WLANs," *Selected Areas in Communications, IEEE Journal on*, vol. 22, pp. 1987-2003, 2004. Article (CrossRef Link)
[36] Yamasaki Y., Shimonishi H. and Murase T., "Statistical Evaluation of TCP Packet Loss Rate Estimation," in *Proc. of Information and Telecommunication Technologies, 6th Asia-Pacific Symposium on*, pp. 23-28, Nov. 10-10, 2005. Article (CrossRef Link)
[37] Prieto J., Bahillo A., Mazuelas S. and Lorenzo, R.M., "Adding Indoor Location Capabilities to an IEEE 802.11 WLAN using Real-Time RTT Measurements," in *Proc. of Wireless Telecommunications Symposium*, pp. 1-7, April 22-24, 2009. Article (CrossRef Link)

[38] Igor Bisio, Fabio Lavagetto, Mario Marchese and Andrea Sciarrone, "GPS/HPS-and Wi-Fi Fingerprint-based Location Recognition for Check-In Applications over Smartphones in Cloud-based LBSs," *Multimedia, IEEE Transactions on*, vol. 15, no. 4, pp. 858-869, 2013. Article (CrossRef Link)
[39] Igor Bisio, Fabio Lavagetto, Mario Marchese and Andrea Sciarrone, "Performance Comparison of a Probabilistic Fingerprint-based Indoor Positioning System over Different Smartphones," in *Proc. of International Symposium on Performance Evaluation of Computer and Telecommunication Systems*, pp. 161-165, July 7-10, 2013. Article (CrossRef Link)
[40] Zhi-An Deng, Ying Hu, Jianguo Yu and Zhenyu Na. "Extended Kalman Filter for Real Time Indoor Localization by Fusing WiFi and Smartphone Inertial Sensors," *Sensors*, vol. 6, pp. 523-543, 2015. Article (CrossRef Link)
[41] McGuire M. and Plataniotis K.N. "Dynamic model-based filtering for mobile terminal location estimation," *Vehicular Technology, IEEE Transactions on*, vol. 52, no. 4, pp. 1012-1031, 2003. Article (CrossRef Link)
[42] Drake and Samuel Picton, "Converting GPS coordinates [phi, lambda, h] to navigation coordinates (ENU)," *DSTO Electronics and Surveillance Research Laboratory*, 2002. Article (CrossRef Link)
[43] Berns H.-G., Burnett T.H., Gran R. and Wilkes R.J., "GPS time synchronization in school-network cosmic ray detectors," *Nuclear Science, IEEE Transactions on*, vol. 51, no. 3, pp. 848-853, 2004. Article (CrossRef Link)

Wanlong Zhao received his B.S. and M.S. from Harbin Institute of Technology, Harbin, China, in 2011 and 2013, respectively. He is currently working toward the Ph.D. degree with School of Electronics and Information Engineering, Harbin Institute of Technology. His research interests include indoor navigation, multi-source data fusion localization and big data.

Shuai Han began his university studies in 2000 in the Communication Engineering from Harbin Institute of Technology. He received his ME and PH.D degree in Information and Communication Engineering from Harbin Institute of Technology in 2007 and 2011, respectively. And he completed his post-doctoral work in 2012 in Electrical and Computer Engineering from Memorial University of Newfoundland in Canada. He is currently an associate professor at Department of Electronics and Communication Engineering, Harbin Institute of Technology. Dr. Han's research interests include wireless sensor networks, wireless communications, the global navigation satellite system; indoor location. He is an associate editor of IEEE Access. He has served as a co-chair for technical symposia of international conference IWCMC 2015, VTC FALL 2016, IWCMC 2016, ComComAp 2012 Workshop. He has also served as the TPC member for many international conferences, including the IEEE ICC, IEEE GLOBECOM, VTC, IEEE COMNETSAT, APCC. Also he is member of IEEE Communication Society, Secretary of IEEE Harbin ComSoc Chapter.

Weixiao Meng received the B.Eng., M. Eng., and Ph.D. degrees from Harbin Institute of Technology (HIT), Harbin, China, in 1990, 1995, and 2000, respectively. From 1998 to 1999, he worked at NTT DoCoMo on adaptive array antenna and dynamic resource allocation for beyond 3G as a senior visiting researcher. He is now a full professor at the School of Electronics and Information Engineering of HIT. His research interests include broadband wireless communications and networking, MIMO, GNSS receiver and wireless localization technologies. He has published 3 books and over 200 papers on journals and international conferences. He is the Chair of IEEE Communications Society Harbin Chapter, a senior member of the IEEE ComSoc, the China Institute of Electronics and the China Institute of Communication. He has been an editorial board member for Wiley's WCMC Journal since 2010, an area editor for PHYCOM journal since 2014, an editorial board for IEEE Communications Surveys and Tutorials since 2014 and IEEE Wireless Communications since 2015. He acted as leading TPC co-chair of ChinaCom2011 and ChinaCom2016, leading Services and Applications track co-chair of IEEE WCNC2013, Awards co-chair of IEEE ICC2015 and Wireless Networking Symposia co-Chair of Globecom 2015. In 2005 he was honored provincial excellent returnee and selected into New Century Excellent Talents (NCET) plan by Ministry of Education, China in 2008.

Deyue Zou received the B.Eng., M.Eng., degrees from Harbin Institute of Technology, Harbin, China, in 2009 and 2011, respectively. He is now a Ph.D. student at the School of Electronics and Information Engineering of Harbin Institute of Technology. His research interests include indoor localization techniques, seamless positioning and GNSS receiver technologies.